Second International Conference on CFD in the Minerals and Process Industries
CSIRO, Melbourne, Australia
6-8 December 1999

MODELLING CONVECTIVE BOILING OF MOLASSES

Darrin W. STEPHENS and Jonathan A. HARRIS

School of Engineering, James Cook University, Townsville, Queensland 4811, AUSTRALIA

ABSTRACT

One- and two-dimensional numerical models of forced convective boiling of molasses in a calandria tube are described. The flow in the tube is considered to be composed of two phases (molasses and steam). The one-dimensional model solves a simplified set of ODEs describing the non-equilibrium boiling process. The two-dimensional model is based on the Eulerian/Eulerian multi-phase approach as implemented in the CFX-4.2 CFD code, and solves for the distribution of volume fraction and the temperature and velocity of each phase, along with global parameters such as pressure drop and evaporation rate.

Solutions are presented for a case with similar conditions to those expected in a batch vacuum pan. The results show that the flow in the tube is complex and multi-dimensional. Vapour forms both at the wall (due to direct heating) as well as in the centre (due to bulk boiling). The observed features of the flow from the numerical simulation are qualitatively similar to available experimental observations made by previous investigators, although quantitative agreement has yet to be achieved.

NOMENCLATURE

C_p	heat capacity
k	thermal conductivity
T	temperature
h_{fg}	heat of vapourisation
T_{sat}	liquid saturation temperature
r	volume fraction
H	enthalpy
p	pressure
S	energy source term
d	bubble diameter
C_D	drag coefficient
$\vec{\mathbf{B}}$	buoyancy force vector
$\vec{\mathbf{u}}$	velocity vector
$\vec{\mathbf{F}}$	body force vector
$\dot{m}$	specific mass transfer rate from liquid to vapour
$\dot{m}_{\alpha\beta}$	coefficient of mass exchange from phase α to β
$c_{\alpha\beta}^{(d)}$	coefficient of momentum exchange from phase α to β
$c_{\alpha\beta}^{(h)}$	coefficient of energy exchange from phase α to β
$h_{\alpha\beta}$	heat transfer coefficient between phase α and β
$A_{\alpha\beta}$	interfacial area between phase α and β
ρ	density
β	thermal expansion coefficient
μ	dynamic viscosity

Subscripts

l	liquid (molasses)
v	vapour (steam)
α	phase α
β	phase β

INTRODUCTION

Vessels used in the processing of raw sugar, such as batch vacuum pans, continuous pans and evaporators, incorporate calandria tube heat exchangers. The tubes are heated externally by condensing steam and the liquid inside the tubes boils. The vapour formed inside the calandria tubes during the boiling process causes a net pressure difference between the tube inlet and outlet and drives a natural circulation up through the tubes and down a central downtake, as shown in Fig. 1. Although the multiphase flow in the calandria tubes largely controls both the circulation and the heat transfer within these vessels, there is little known about its exact nature for viscous fluids, such as syrup, molasses and massecuite (a mixture of molasses and crystals).

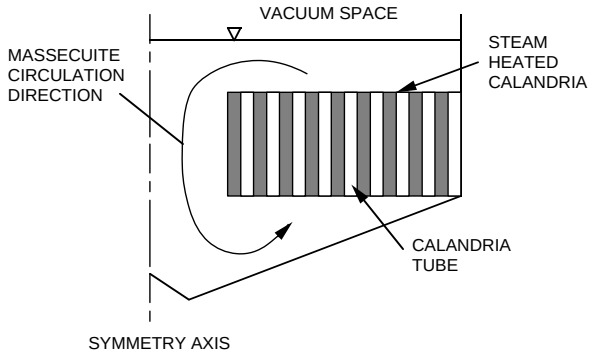

Figure 1: Cross section through a typical vacuum pan

Due to the high viscosity of these fluids, convective boiling in calandria tubes generally takes place in the laminar flow regime. Rouillard (1985a) performed a comprehensive experimental study of forced convective boiling of syrup, molasses and massecuite and developed correlations for the pressure drop and heat transfer coefficients in the calandria tubes. However, simple pan circulation models based on these correlations show considerable scatter when compared with measured evaporation rates (Rouillard, 1985b), suggesting that improvements in both the modelling and

correlations are possible. Also, the use of the condensate flow rate to determine the overall heat transfer to the massecuite in the experiments is open to question, since it does not account for heat losses. Other experimental investigations in the area of sugar boiling have been performed by Austmeyer and Schliephake (1983) and Austmeyer (1986) who studied low viscosity sugar solutions. They observed that, for their highest viscosity solution, a vapour blanket formed on the pipe wall in the upper portion of the tube (inverted annular flow) which hindered heat transfer. They also found significant radial and axial variation in temperature, velocity and supersaturation within the tube.

Models of circulation in vacuum pans (e.g., Rouillard, 1987) require a knowledge of the vapour formation and pressure drop in calandria tubes. Even some recent papers, such as Sheng (1993), have improperly assumed that single-phase pressure drop relationships are applicable within calandria tubes. Such assumptions can lead to gross errors in prediction of circulation in pans.

Some limited computational fluid dynamics (CFD) modelling of simplified vacuum pans has been performed (Bunton, 1981; Brown *et al*., 1992). Neither of these studies properly modelled the flow within the calandria tubes. For example, Bunton (1981) considered the pressure drop in the calandria tubes to be given by single-phase laminar flow, which is clearly inappropriate. Brown *et al*. (1992) only simulated the forced circulation of massecuite in single-phase flow under isothermal conditions which is not representative of natural circulation in pans.

In this paper one and two-dimensional models of the two-phase flow in a single calandria tube are presented and discussed. The simulation results show the processes which occur in calandria tubes under similar conditions to those found in a vacuum pan. Once validated, these model can also be used to generate improved correlations for pressure drop, evaporation rates and heat transfer in calandria tubes. The modelling techniques developed here will find future application in predicting circulation in vessels with calandria tube heat exchangers, such as vacuum pans.

MATHEMATICAL MODEL DESCRIPTION

Eulerian two-phase flow model

The axisymmetric model geometry consists of a single calandria tube of length 1 m and internal diameter 100 mm, as shown in Fig. 2. These dimensions are representative of calandria tubes used in batch vacuum pans.

The two-phase model is based on an Eulerian approach in which each phase is assumed to interpenetrate with the other and occupy a certain volume fraction of each computational cell. For the present model the phases are molasses and vapour, and the flow is assumed to be at steady state. The governing equations are conservation of mass, momentum and energy for each phase and are presented in chapter 12 of the CFX-4.2 solver manual (CFX International 1997). Additional equations are required to describe the transfer of mass, momentum and energy between phases and at the wall.

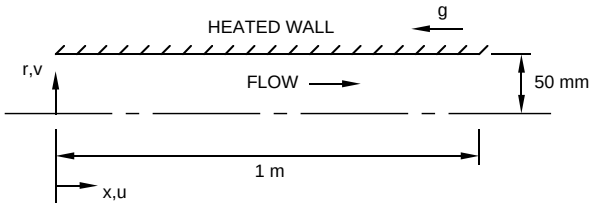

Figure 2: Geometry of tube model

For two phases the sum of the volume fractions at a point must equal unity, viz:

$$\sum_{\alpha=1}^{2} r_\alpha = 1 \tag{1}$$

The steady state continuity equation for phase α is

$$\nabla \cdot \left(r_\alpha \rho_\alpha \vec{\mathbf{u}}_\alpha\right) = \sum_{\beta=1}^{2} \left(\dot{m}_{\alpha\beta} - \dot{m}_{\beta\alpha}\right) \tag{2}$$

The steady state conservation of momentum equation for phase α is

$$\begin{aligned} &\nabla \cdot \left(r_\alpha (\rho_\alpha \vec{\mathbf{u}}_\alpha \otimes \vec{\mathbf{u}}_\alpha - \mu_\alpha (\nabla \vec{\mathbf{u}}_\alpha + (\nabla \vec{\mathbf{u}}_\alpha)^T))\right) = \\ &r_\alpha \left(\vec{\mathbf{B}}_\alpha - \nabla p\right) + \sum_{\beta=1}^{2} c_{\alpha\beta}^{(d)} \left(\vec{\mathbf{u}}_\beta - \vec{\mathbf{u}}_\alpha\right) + \\ &\sum_{\beta=1}^{2} \left(\dot{m}_{\alpha\beta} \vec{\mathbf{u}}_\beta - \dot{m}_{\beta\alpha} \vec{\mathbf{u}}_\alpha\right) + \vec{\mathbf{F}}_\alpha \end{aligned} \tag{3}$$

where the pressure is common to both phases. The conservation of energy equation for phase α is

$$\begin{aligned} &\nabla \cdot \left(r_\alpha (\rho_\alpha \vec{\mathbf{u}}_\alpha H_\alpha - k_\alpha \nabla T_\alpha)\right) = \sum_{\beta=1}^{2} c_{\alpha\beta}^{(h)} \left(T_\beta - T_\alpha\right) + \\ &\sum_{\beta=1}^{2} \left(\dot{m}_{\alpha\beta} H_\beta - \dot{m}_{\beta\alpha} H_\alpha\right) + S_\alpha \end{aligned} \tag{4}$$

The interfacial momentum exchange coefficient is given by

$$c_{\alpha\beta}^{(d)} = \frac{3}{4} C_D \frac{r_\alpha \rho_\alpha \left|\vec{\mathbf{u}}_\beta - \vec{\mathbf{u}}_\alpha\right|}{d} \tag{5}$$

where the the drag coefficient is determined by Stokes law (Stokes, 1901). The interfacial heat exchange coefficient is expressed as

$$c_{\alpha\beta}^{(h)} = h_{\alpha\beta} A_{\alpha\beta} \tag{6}$$

where the heat transfer coefficient is computed using the correlation of Ranz and Marshall (1952a, b). Interfacial mass transfer is proportional to the heat transfer between the two phases.

Information required at the wall includes the nucleation site density, frequency of bubble detachment from the wall, bubble size at detachment, and the superheat required for activation of nucleation sites. All of these parameters involve uncertainty for molasses, and at present have been assigned values based on the available literature and "educated guesses". The sensitivity of the model to these values will be assessed in the future. Various modifications were required to the source code of the boiling model currently implemented in CFX-4.2. These modifications include changes to the wall heat partitioning model and allowing the saturation temperature to vary with height due to the change in hydrostatic pressure.

The equations are solved using the finite volume method and the IPSAC procedure. A false transient method was used to obtain the steady-state solution. Under-relaxation factors of 0.4 , 0.65 and 1.0 were used for the volume fraction, momentum and energy equations, respectively. The mass transfer was also under-relaxed using a factor of 0.01. Further details of the governing equations and solution methods are given by CFX International (1997).

The boundary conditions for the simulation are a prescribed uniform wall heat flux (1 kW/m^2), a mass flow rate (0.717 kg/s) with a parabolic velocity profile at the inlet, a uniform molasses temperature (347.15 K) at the inlet, no-slip conditions on the tube wall, and fully developed flow at the outlet. Additionally, the variation in saturation temperature along the axis of the tube had to be specified. The saturation temperature was calculated from the absolute pressure that the fluid would experience within Rouillard's (1985a) experimental apparatus, i.e. calculated from the height of molasses above the tube top and the pressure above the free surface. For this simulation the value used for the height of molasses is 0.3 m and the pressure above the free surface is 24.5 kPa (absolute). This gives a range for the saturation temperature between 353.5 and 346.5 K.

Properties of the molasses correspond to that used in Roulliard's (1985a) experimental run 7 and are ρ_l = 1457 kg/m^3, ρ_v = 1 kg/m^3, k_l = 0.4 W/m.K, k_v = 21.7×10^{-3} W/m.K, C_{pl} = 1775 J/kg.K, μ_l =0.745 Pa.s, μ_v = 489×10^{-6} Pa.s and h_{fg} = 2358 kJ/kg. Buoyancy effects due to heating are also included using the Boussinesq approximation with a coefficient of thermal expansion β = 3.0017×10^{-3} K^{-1}. The molasses is assumed to be Newtonian with a viscosity independent of temperature, which is not the case in reality. However, a more realistic viscosity model will be introduced at a later stage. A uniform bubble diameter of 1 mm was assumed in the heat and momentum transfer correlations.

For the results presented here the computational mesh consists of 350 volumes in the axial direction and 25 volumes in the radial direction. The mesh is biased in the radial direction closer to the wall to resolve the narrow boundary layers, whilst the spacing in the axial direction is biased towards the tube outlet since this is where the majority of the phase change occurs. With any simulation it is important to assess the effect of mesh refinement (Freitas, 1993). A grid-independence check was performed using 400 x 40 volumes in the axial direction and radial directions, respectively. The total energy at the outlet of the tube changed by less than 0.1% so that the solution on the original mesh is considered essentially grid-independent.

The simulation was carried out on James Cook University's SGI Power Challenge supercomputer using one R10000 CPU. The total time for the simulation with the 350 x 25 mesh was 22 CPU hours.

One-dimensional, two-phase flow model

Although it yields detailed results, the two-dimensional model takes a considerable time to run. Thus, it is not well suited to parametric studies of the flow behaviour as a function of applied heat flux and mass flow rate. In this section a simplified one-dimensional, two-phase flow model is presented that sacrifices solution detail in favour of short run times.

Assume one-dimensional flow occurs so that all quantities have uniform profiles at any streamwise position along the tube. Under this assumption the continuity equations simplify to

$$\begin{aligned} \frac{d}{dx}\left((1-r_l)\rho_v u_v\right) &= \dot{m} \\ \frac{d}{dx}\left(r_l \rho_l u_l\right) &= -\dot{m} \end{aligned} \tag{7}$$

where is $\dot{m}$ the mass transfer per unit volume from the liquid to the vapour. The one-dimensional momentum equations are

$$\begin{aligned} -(1-r_l)\frac{dp}{dx} + u_l\dot{m} + c_{vl}^{(d)}(u_l - u_v) &= \frac{d}{dx}\left((1-r_l)\rho_v u_v^2\right) \\ -r_l\frac{dp}{dx} - u_l\dot{m} + c_{lv}^{(d)}(u_v - u_l) &= \frac{d}{dx}\left(r_l\rho_l u_l^2\right) \end{aligned} \tag{8}$$

In the above momentum equations the axial shear stress has been omitted as it is small compared with the other terms. Neglecting axial conduction, which is a valid assumption for the high Peclet number flow considered here, the one-dimensional energy equations are

$$\begin{aligned} \frac{d}{dx}\left((1-r_l)\rho_v u_v H_v\right) &= c_{vl}^{(h)}(T_l - T_v) + \dot{m}H_l \\ \frac{d}{dx}\left(r_l\rho_l u_l H_l\right) &= c_{lv}^{(h)}(T_v - T_l) + \dot{m}H_v \end{aligned} \tag{9}$$

Following Stephens and Harris (1988), equations (7), (8) and (9) may be rearranged to yield a set of ordinary differential equations in the six unknowns ρ_l, u_l, u_v, p, H_v and H_l. Given the thermofluid properties of each phase, a saturation temperature profile and appropriate inlet conditions, these equations may be integrated along the tube to yield axial profiles of the unknown variables. Here, the integration was carried out using the Matlab^{TM} routine ode15s for stiff

ODEs. The inlet conditions and thermofluid properties were taken to be the same as the two-dimensional model, except where noted below.

The one-dimensional model cannot account for frictional pressure drop in the tube. However, this can be computed separately by using correlations to determine the two-phase flow friction factor.

RESULTS

Eulerian two-phase flow model

The Eulerian two-phase flow model outputs the distribution of temperature, velocity, pressure and volume fraction for each phase (molasses and vapour). From these detailed results it is also possible to compute global quantities of interest such as overall pressure drop, heat transfer and evaporation rate.

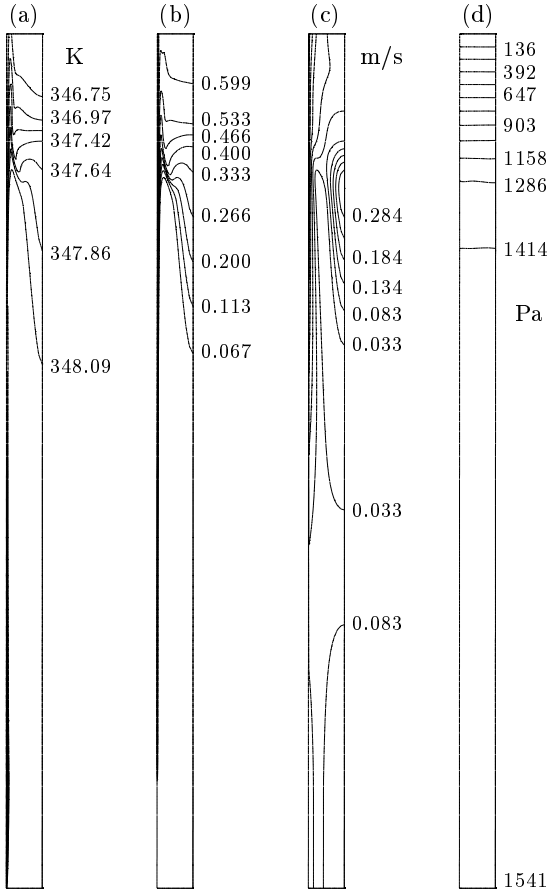

Figure 3: Two-dimensional model results. Flow is from bottom to top, the tube wall is on the left and the tube axis is on the right of each figure. (a) liquid temperature; (b) vapour volume fraction; (c) liquid velocity; (d) pressure.

Results of the model are shown in Fig. 3 (a) to (d) for the conditions given above. There are three classical zones visible in these figures: single-phase heating, sub-cooled boiling, and bulk boiling (Collier and Thome, 1996). The relative size of these zones depends strongly on the mass flow rate, wall heat flux and saturation temperature profile.

In the single-phase heating zone no boiling occurs. The flow enters the tube, is heated at the wall and a very thin thermal boundary layer develops next to the wall as shown Fig. 3 (a). Note that the very thin thermal boundary layer is due to the very high Prandtl number of the molasses. There is essentially no vapour phase present at this point. As can be seen in Fig. 3 (c) the velocity profile near the inlet follows the expected parabolic shape for fully developed laminar flow in a pipe. About one-fifth of the way along the tube sub-cooled boiling commences. In this zone boiling occurs immediately adjacent to the wall where the liquid temperature has reached saturation temperature. The thermal boundary layer at the wall thins and vapour is formed very near the wall. The vapour formation at the wall accelerates the flow near the wall and, by conservation of mass, the velocity in the centre of the tube slows, eventually to virtually zero (i.e., the region inside the 0.033 m/s contour).

Approximately two-thirds of the way along the tube the prescribed saturation temperature, which is dependent on the vertical elevation, falls to equal the temperature of the molasses in the centre part of the tube. At this point bulk boiling occurs and a great deal of vapour is formed as shown in Fig. 3 (b). The bulk vapour formation accelerates the flow in the centre part of the tube as shown in Fig. 3 (c). This acceleration causes the majority of the pressure drop as shown in Fig. 3 (d). Even when there is a high volume fraction of vapour, the vapour and molasses still move at virtually the same speed due to the high viscosity of the molasses which results in a very large drag between the two phases.

These results are consistent with the observation by Austmeyer and Schliephake (1983) of a vapour blanket at the wall in the upper part of the tube. The presence of this vapour layer is detrimental to heat transfer from the wall to the fluid. However, it does speed the flow adjacent to the wall, which reduces the velocity in the centre part of the tube, allowing time for vapour to form. This is an important two-dimensional effect. Indeed, the one-dimensional boiling model described above shows that there is insufficient time for bulk vapour formation if the velocity is not slowed in this manner (refer to following section).

In this simulation the applied wall heat flux (1 kW/m^2) was much lower than the reported measured heat flux of Rouillard (1985a) of 18 kW/m^2. At this stage in the research it is still not possible to simulate wall heat fluxes that are representative of conditions in a vacuum pan, but this limitation is currently being addressed.

For this simulation the overall pressure drop is about 1.5 kPa which is significantly larger than that for single-phase flow of molasses at the same mass flow rate (240 Pa). The difference is due to the acceleration caused by vapour formation. The average volume fraction of vapour leaving

the tube is about 0.64 which yields an overall evaporation rate of 3.9 kg/h. This value is comparable to, but somewhat less than, the evaporation rate found in a batch vacuum pan (approximately 10 kg/h per tube). The predicted rate is lower than that generally observed due to the low applied wall heat flux mentioned above.

One-dimensional two-phase flow model

Results from the one-dimensional model are presented in Fig. 4, along with some experimental data and radially averaged two-dimensional model results for comparison.

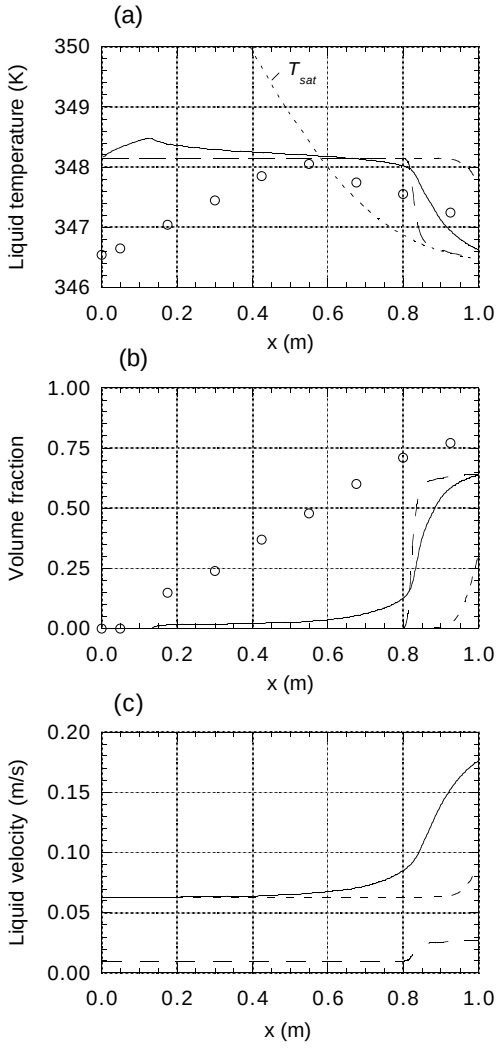

Figure 4: One-dimensional model results. Short and long dashes correspond to inlet velocities of 0.063 m/s and 0.01 m/s, respectively. Solid line is radial average of the two-dimensional results shown in Fig. 3. Data points are from Rouillard (1985a) experimental run 7: in (a) the measurements are at the tube axis, whereas in (b) the measurements are volume averages across the tube.

There are two curves shown for the one-dimensional model. The first is for a bulk inlet velocity of 0.063 m/s, which corresponds to the mass flux used in the two-dimensional model and the experimental run, and the second is for an artificially reduced velocity of 0.01 m/s.

It is important to realise that the models have different wall heat fluxes: the one-dimensional model has zero heat flux (although this could easily be added); the two-dimensional model has a wall heat flux of 1 kW/m^2; and the reported heat flux for the experimental run is 18 kW/m^2. As presented, the one-dimensional model only models the vapour formation due to flashing, when the bulk temperature exceeds the saturation temperature.

The inlet temperatures for the one-dimensional model are set higher than the experimental run since the single phase heating zone is not modelled (if it were the bulk temperature would increase linearly from the inlet). The axial temperature profiles from the one-dimensional model clearly demonstrate non-equilibrium effects. That is, the liquid becomes superheated for a portion of the tube ($x > 0.6$ m) before flashing to vapour. In the higher velocity case the superheated region extends to the end of the tube, whereas in the lower velocity case the flow has time to attain thermal equilibrium before the end of the tube. Consequently, the lower inlet velocity case exhibits significantly more vapour formation due to flashing than the higher inlet velocity case.

The radially-averaged axial temperature profile from the two-dimensional model does exhibit some bulk heating due to the imposed heat flux. However, once sub-cooled boiling occurs the bulk temperature decreases since the saturation temperature decreases. Since the tube outlet temperature is less than the inlet temperature this flow would not sustain natural circulation.

DISCUSSION

In order for a mathematical model of the tube boiling to be successful it must properly describe both the subcooled and bulk boiling zones. These zones are highly two-dimensional so it seems reasonable to expect that a two-dimensional model will be superior to a one-dimensional model.

The two-dimensional model does predict sub-cooled boiling. However, at this stage it does not produce results that are representative of available experimental data. The data of both Rouillard (1985a) and Austmeyer (1986) show a noticeable increase in the temperature at the axis of the tube in the sub-cooled flow region (e.g., see Fig. 4 (a)). This could only occur if there is some heat transfer mechanism (e.g., bulk mixing caused by bubble blockage effects, or "heat pipes" formed by bubbles protruding from the hot wall into the cooler fluid) that allows heat to be transferred to the tube axis. At present such mechanisms are not included in the Eulerian two-fluid two-phase flow model, since the bubbles are not explicitly represented, with the result that all the heating and vapour formation are confined to an extremely narrow wall region. Attempts to increase the wall heat flux to realistic values causes the code to fail as the

volume fraction at the wall approaches unity and there is no mechanism for the energy to get away from the wall. In contrast, the one-dimensional model would be able to represent the bulk fluid heating in the sub-cooled zone as the heat flux would be implemented as a volumetric source term in the liquid energy equation. Of course, the one-dimensional model would predict no vapour formation in the sub-cooled region which is not realistic.

In the bulk boiling region the two-dimensional model performs well. Notably, it predicts the slowing of the flow near the axis which is essential to allow sufficient time for bulk boiling to occur. As the one-dimensional model is incapable of representing this two-dimensional effect it fails to properly model the bulk boiling region. Only when the inlet velocity is artifically reduced by a factor of more than 6 does the one-dimensional model begin to capture the bulk boiling zone.

The non-equilibrium one-dimensional model could not be used for prediction of vapour formation without modification as it fails to predict the bulk boiling zone. It may be the case that a simpler model assuming thermodynamic equilibrium would better capture the bulk boiling region, although it is likely to overpredict the amount of vapour generated.

The two-dimensional model holds the most promise for predicting this flow, but does require modification in the sub-cooled region since it currently does not allow sufficient heat to be transferred from the wall region to the centre of the tube.

CONCLUSION

Numerical models of the convective boiling of molasses in a calandria tube under laminar flow conditions have been presented. For conditions similar to those in a batch vacuum pan the two-dimension model results exhibit regions of sub-cooled boiling and bulk boiling. There are significant radial variations of temperature, velocity and volume fraction and a noticeable vapour blanket formed at the wall near the tube outlet. The vapour and liquid phases both travel at virtually the same velocity due to large drag of the high viscosity molasses. The one-dimensional model is simple and runs quickly, but fails to adequately predict the bulk vapour formation without using an artificially low inlet velocity. Compared with the experimental data, but both models underestimate the amount of vapour formed in the lower part of the tube.

It should be noted that the results are only given for one set of parameters and vary greatly with applied heat flux, mass flow rate, inlet conditions and saturation temperature. Additionally, the two-dimensional model results could change significantly once a more realistic viscosity model (i.e., temperature dependent and pseudoplastic) and a higher wall heat flux are introduced.

REFERENCES

AUSTMEYER, K.E., (1986), "Analysis of sugar boiling and its technical consequences: Part II. Heat Transfer during sugar boiling". *Int. Sugar J*., **88**, 23-29.

AUSTMEYER, K.E. and SCHLIEPHAKE, D., (1983), "Solution flow and exchange and heat transfer in a heating tube of an evaporation-crystallizer*". Int. Sugar J*., **85**, 328-333.

BUNTON, J.J., (1981), "Natural convection, two-phase flow and crystallization in a vacuum pan sugar crystallizer". PhD Thesis, Louisiana State University.

BROWN, D.J., ALEXANDER, K. and BOYSAN, F., (1992), "Crystal growth measurement and modelling of fluid flow in a crystallizer". *Zuckerind* **117** (1) 35-39.

CFX INTERNATIONAL (1997), CFX Solver Manual. V4.2. 8.19 Harwell, Didcot, Oxfordshire, United Kingdom.

COLLIER, J.G. and THOME J.R., (1996), "Convective boiling and condensation", 3rd edition, Oxford University Press.

FREITAS, C.J., (1993), Editorial. *J. Fluids Eng*. **115** 339.

RANZ, W.E. and MARSHALL, W.R. Jr., (1952a), "Evaporation from Drops, Part 1". *Chem Eng Prog*. **48** (3) 141-146.

RANZ, W.E. and MARSHALL, W.R. Jr., (1952b), "Evaporation from Drops, Part 2". *Chem Eng Prog.* **48** (4) 173-180.

ROUILLARD, E.E.A., (1985a), "A study of boiling parameters under conditions of laminar non-Newtonian flow with particular reference to massecuite boiling". PhD thesis, University of Natal.

ROUILLARD, E.E.A., (1985b), "Massecuite boiling". *Proc. SASTA*, 43-47.

ROUILLARD, E.E.A., (1987), "Some ideas on the design of batch and continuous pans". *Proc. SASTA*, 76-82.

SHENG, L.Q., (1993), "Determining the circulation ratio of pans". *Int. Sugar J*., **95**, 183-186.

STEPHENS, D.W. and HARRIS, J.A., (1998), "Numerical modelling of two-phase flow: a benchmark solution". *Proc. 13th Aust. Fluid Mech. Conf*., Melbourne.

STOKES, G.G., (1901), Mathematical and Physical Papers, vol. III, p. 55, Cambridge University Press.